SURFACE PIERCING PROPELLERS
- METHODICAL SERIES MODEL TEST RESULTS -

1. INTRODUCTION

In recent years the number of high-speed craft propelled by surface piercing propellers has increased substantially. There are now several thousand vessels operating with surface piercing propellers, including sophisticated high performance naval vessels and long distance record breakers. Surprisingly, however, very little data has been published which permits to select optimum propeller dimensions and which indicates the magnitude of propeller vertical and side forces, with their usually significant effects on craft performance. Sizing of surface piercing propellers is largely done empirically, even if a few designers have developed great expertise and accumulated an impressive know-how. Philip Rolla of *Rolla SP Propellers SA*, Switzerland is probably the best known and most experienced one among them. Thanks to his initiative and support the authors were in a position to test, at model scale, a limited series of surface piercing propellers, making use of the high-speed free-surface cavitation tunnel of *Technische Universität Berlin*.

2. TEST PROGRAM

2.1 Model Propellers

The propeller series consists of five 4-bladed propellers (Fig. 1), all having a blade-area ratio of A_e/A_o = 0.80 and pitch-diameter ratios of P/D = 0.9, 1.1, 1.2, 1.4, 1.6. The model propellers had diameters of D = 250 mm, the propeller material was aluminium with anodized surface finish. The type of blade section used in all propellers can be seen from Fig. 2, displaying little camber but substantial trailing edge cupping. The propeller design represents a well-proven, commercially available *Rolla* design. It was originally developed for craft of moderate speed capability ($35 \leq V_S \leq 45$ knots) that would benefit from propeller lifting forces. In actual fact, full scale application of this design has had a much wider spreading ($20 \leq V_S \leq 70$ knots). The choice of using a proven current design for the methodical investigation was to develop a sound data base for a continuing testing and design program.

2.2 Test Set-up

The propeller tests were carried out in the free-surface cavitation tunnel K 27 of the *Institut für Schiffs- und Meerestechnik* of *Technische Universität Berlin*, making use of the high-speed test

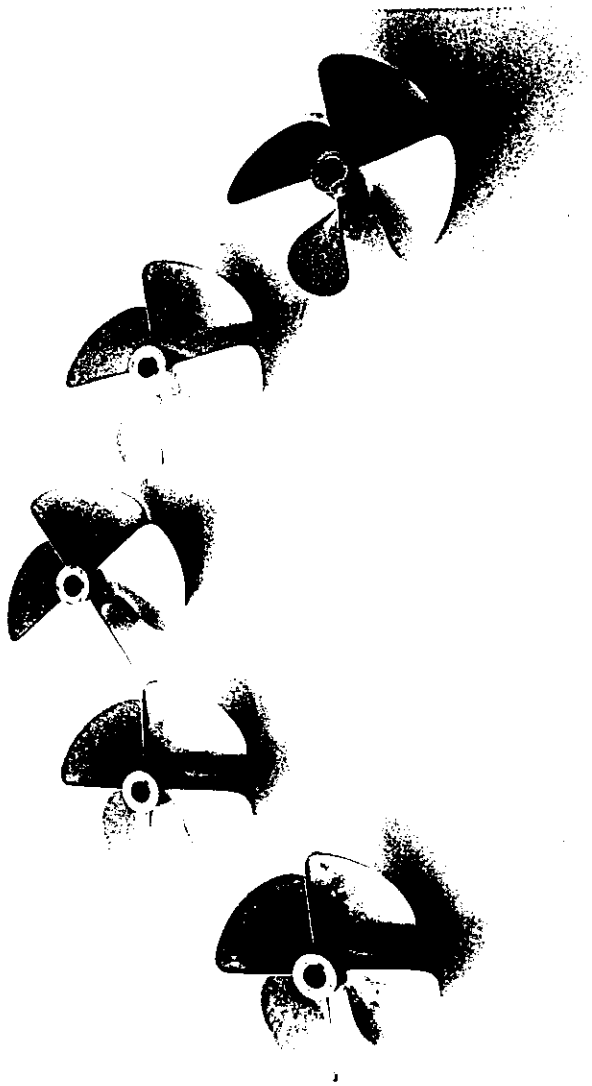

Fig. 1 Rolla Propeller Series

Fig. 2 Blade Section at non-dimensional Radius r/R = 0.7

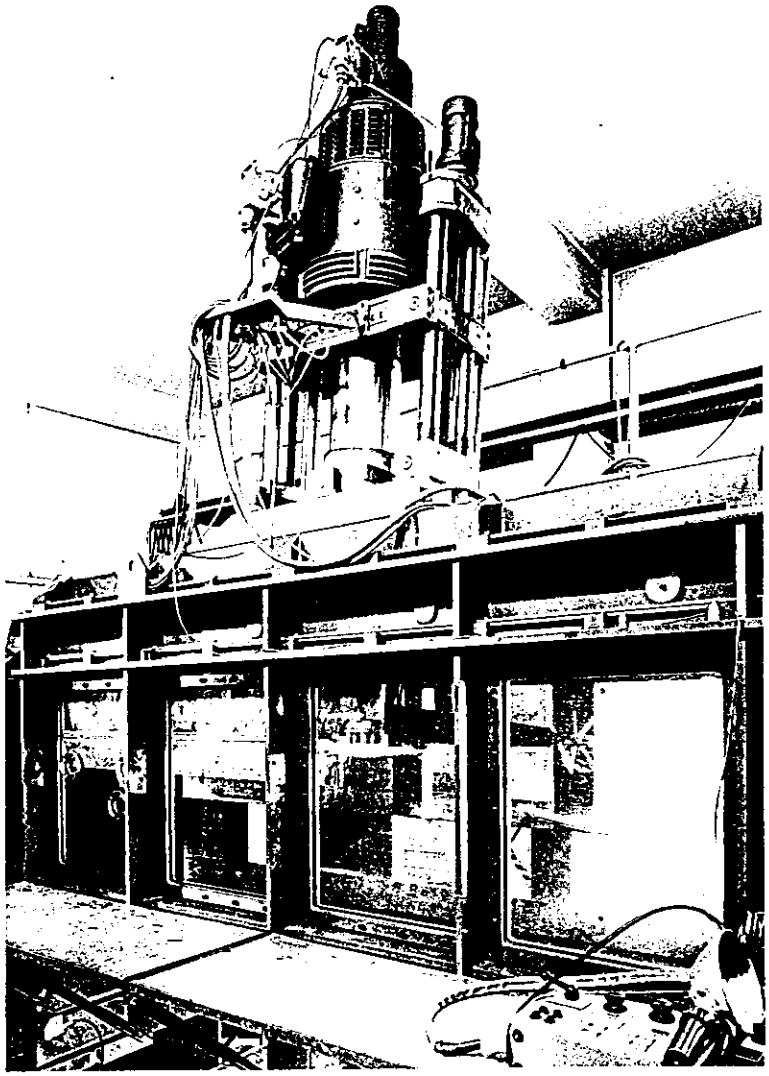

Fig. 3 Test Section of Cavitation Tunnel K27

section with a cross sectional area of 600 x 600 mm^2 (Fig. 3) The propellers were driven by the 6-component right-angle dynamometer, in a position behind a flat plate covering the free surface (Fig. 4). The propeller plane was located at a distance of 2D downstream of the cover plate when a shaft inclination of 8 deg. was maintained. Due to the dynamometer kinematics this distance was moderately changed for different shaft inclinations (see Fig. 4). In full scale, a distance of 2D is also usually required if the feature of propeller shaft articulation is to be achieved. In addition, such a

distance must be maintained to allow the occurence of the surface elevation in front of the propeller at high thrust loading.

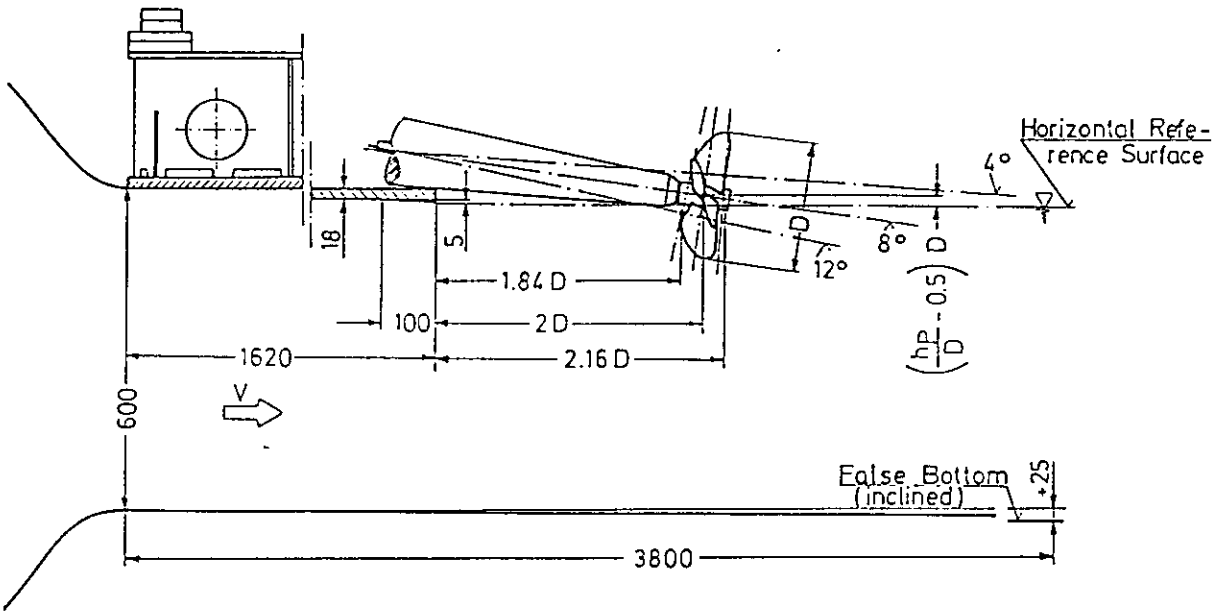

Fig. 4 Details of Test Set-up

Owing to the housing dimensions of the dynamometer drive shaft only limited immersion ratios could be geometrically verified, for given shaft inclinations. These restrictions lead to the set of geometrical combinations for the test program given in Table 1.

Table 1

Shaft Inclination [deg.]	4	8	12
Immersion Ratio [%]	30	47.4	58

At a distance of 2D downstream of the cover plate the velocity distribution in the test section was assessed by means of Pitot-static tube measurements, in the vicinity of the free surface (Fig. 5). In view of large fluctuations in the immediate vicinity of the free surface upper and lower limits were identified of which the higher ones tended to be more stable. On the basis of these velocity distributions mean nominal wake fractions can be defined as volumetric averages over a hypothetically immersed propeller disc area. It should be realized, however, that mean wake fractions determined in this way depend on the model propeller diameter. For a diameter of D = 250 mm the results have been plotted in Fig. 6, both for the upper and lower boundary of Fig. 5.

With the type of test set-up just described it was intended to represent actual full scale positions of propellers in successful practice. A flat plate, here referred to as cover plate, is used to represent the bottom of the vessel. The wake influence, though not proven to be identical, is also present in full

scale craft. The combinations of shaft inclination and immersion ratio are restricted by dynamometer size, but shafting installations in full scale craft are also subject to similar limitations.

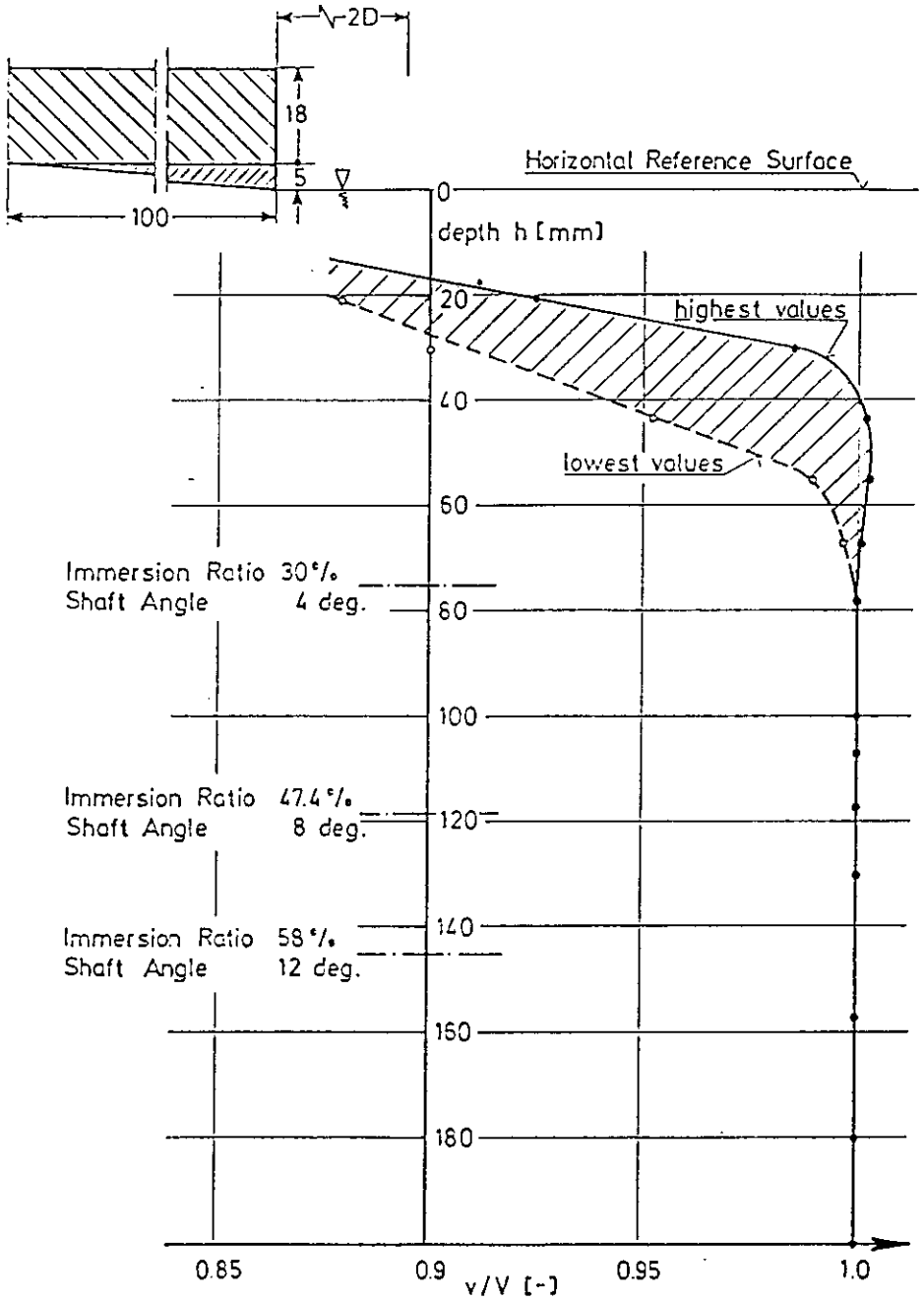

Fig. 5 Velocity Profile in Propeller Plane

2.3 Test Parameters and Procedures

Apart from the variation of the geometric parameters given in Table 1 cavitation number was the prime variable for a given test set-up. This was defined at the free surface to be

$$\sigma = \frac{p_o - p_v}{\frac{\varrho}{2} V^2},$$

where p_o represents the static pressure above the free surface in the tunnel. All tests were carried out under atmospheric pressure conditions in the tunnel (σ_{atm} = sigma atmos.) as well as $\sigma = 0.5$ and $\sigma = 0.2$.

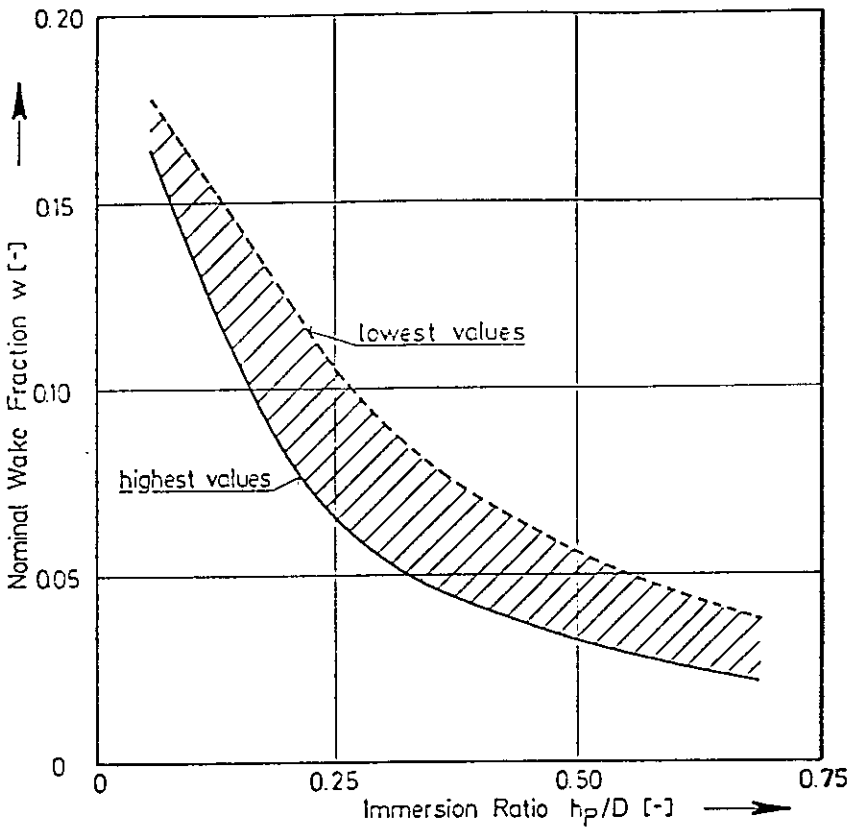

Fig. 6 Wake Characteristics in Propeller Plane

The 6-component propeller dynamometer permits to measure the forces F_a, F_x and F_y defined in Fig. 7. The horizontal propeller thrust must therefore be derived from

$$T = F_a \cos \alpha - F_x \sin \alpha .$$

The upward vertical propeller force on the other hand, is obtained from

$$F_v = F_a \sin \alpha + F_x \cos \alpha .$$

All force coefficients are defined in accordance with ITTC recommendations, e.g.

$$K_T = \frac{T}{\varrho n^2 D^4} , \qquad K_Q = \frac{Q}{\varrho n^2 D^5} , \qquad K_{Fv} = \frac{F_v}{\varrho n^2 D^4} .$$

Efficiencies quoted are likewise based on the horizontal thrust

$$\eta = \frac{TV}{2\pi n Q} .$$

Presenting inclined shaft propeller characteristics in the form of horizontal thrust and quoting efficiencies derived on the same principle is in accordance with standard ITTC practice. Only in this way can one relate propeller thrust and vehicle drag and draw meaningful conclusions about propeller/hull interaction. Frequent propeller sales practice, quoting pure axial flow data and higher efficiencies derived on this basis, is neither useful nor sound and should be discarded.

Another bad custom is to quote efficiencies for the inclined shaft based on the axial shaft force (F_a) rather than on the horizontal thrust (T). This yields higher face values of efficiency as can be understood from Fig. 7. Related full scale trials, however, will unavoidably show disappointing discrepancies which usually remain unexplained.

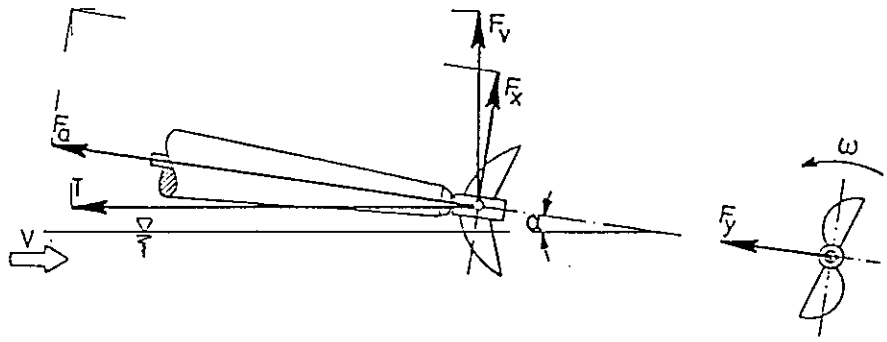

Fig. 7 Propeller Forces on Inclined Shaft

The reference speed V is always the velocity measured in the tunnel at the position of the propeller, at some distance below the free surface (see Fig. 5). All tests were carried out at V = 8 ms^{-1}, the lowest advance coefficient J = V/nD being determined by dynamometer limitations ($n_{max} \approx 2500$ min^{-1}). In order to investigate high propeller thrust conditions, tests were extended into regions of lower advance coefficients at V = 5 ms^{-1}, however only under atmospheric pressure conditions in the tunnel.

Test procedures were such that, for a given geometric configuration, water speed and cavitation number, the propeller advance coefficient was slowly varied from the condition of maximum rotational speed to the zero thrust condition. The resulting force coefficients were plotted on-line and stored on disc. Fig. 8 represents a typical on-line record showing the effect of water speed and cavitation number.

3. TEST RESULTS

3.1 Design Charts

In a usual design process, where limited information on craft performance is available, the most frequent design parameter which can easily be identified is the force coefficient K_Q/J^5. This basis

has therefore been selected to present the test data for the 3 geometric configurations of Table 1 (Fig. 9.....11). Efficiency and advance coefficients are given for the cavitation number $\sigma = 0.5$, as this is related to the most frequent range of application of the type of propeller investigated (see Section 2.1). The data points given in Fig. 9.....11 represent a random selection from results obtained in the form of Fig. 8, taking usually every third of the total measuring points stored on disc.

3.2 Secondary Propeller Forces

Vertical forces on surface piercing propellers usually reach extreme values at low cavitation numbers. It was therefore decided to present vertical force ratios for the geometric conditions of Table 1 (Fig. 12.....14), again on the basis of the force coefficient K_Q/J^5, for $\sigma = 0.2$.

3.3 Thrust Limitations

Under conditions of fully ventilated flow cavitation number has no influence on the magnitude of propeller forces, and hence on efficiency. The test results obtained for atmospheric pressure conditions in the tunnel were therefore plotted on the basis of thrust loading (K_T/J^2), for the geometric conditions of Table 1 (Fig. 15.....17). Whereas the data at moderate thrust loading were obtained with the tunnel speed set at $V = 8\ ms^{-1}$, the higher thrust loading relates to the tests at $V = 5\ ms^{-1}$. Minor discontinuities can be observed at the transition. These are the result of unavoidable tunnel wall effects.

4. DISCUSSION OF RESULTS

The presentation of the model propeller test results in the form of Fig. 9.....11 permits a quick estimate of optimum diameters and associated pitch-diameter ratios of surface piercing propellers, for the design speed range $35 \leq V_S \leq 45$ knots. Upper limits of propeller lift forces for these propellers can be estimated from Fig. 12.....14. Thrust loading limitations that may cause concern around hump conditions can be deduced from Fig. 15.....17.

Experienced users of the design charts will undoubtedly notice, sooner or later, some discontinuities in the results, as a function of pitch-diameter ratio. These are neither caused by measuring errors during the tests, nor by manufacturing tolerances, as far as blade geometry with the exception of the trailing edges is concerned. Degree and application of cupping, however, are not entirely accurate and were finally identified as the reason for said discontinuities.

One of the major conclusions to be drawn from the test results relates to the magnitude of propeller lift forces, for mean and high shaft angles combined with light propeller loading. The latter occurrs when propellers have larger than optimum diameters, or generally for high pitch-diameter ratios. In these cases lift forces cause propeller efficiencies to drop with reduced loading (see Fig. 11). Such a phenomenon is unknown in axial flow propeller performance where a reduction in propeller loading always improves propeller efficiency.

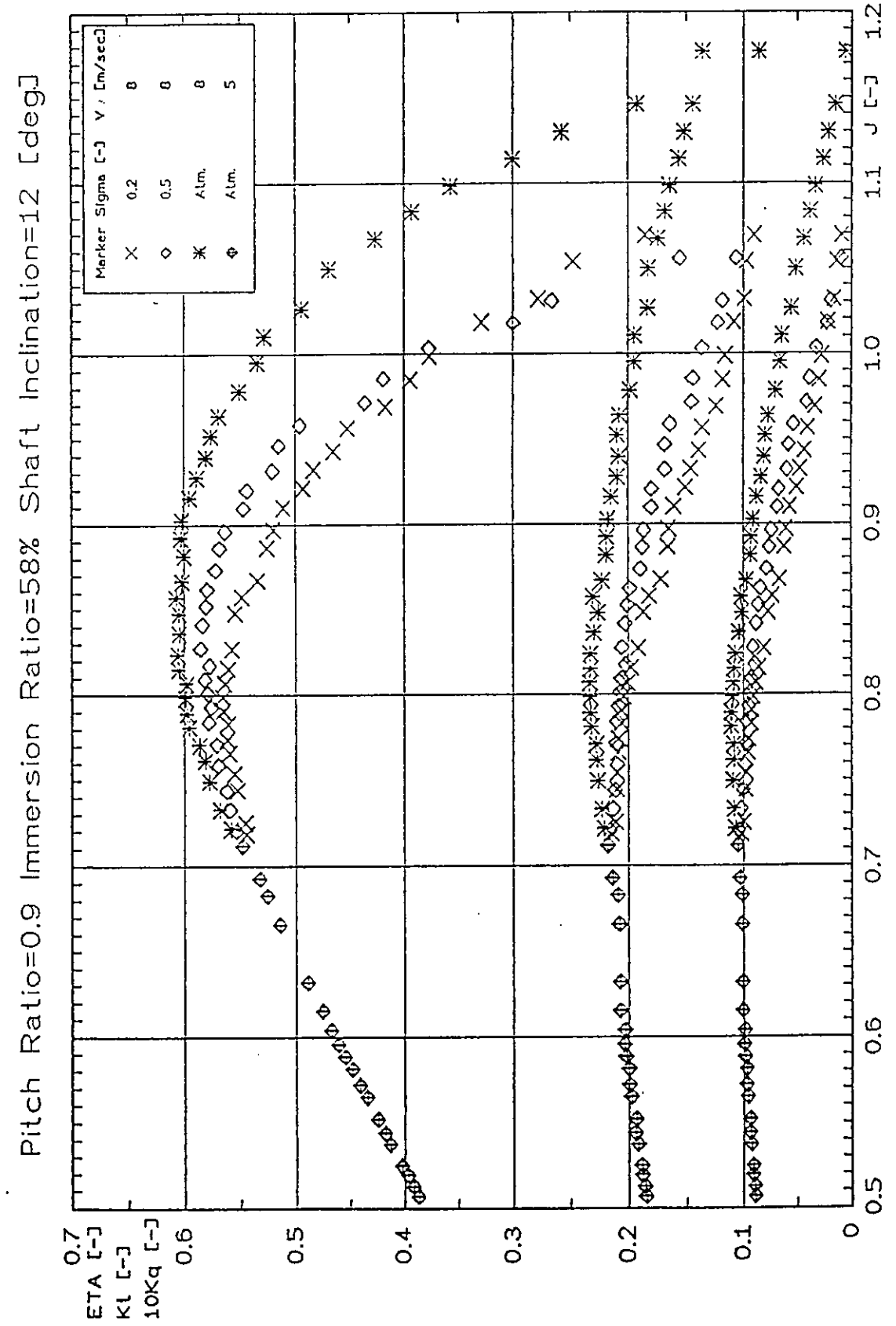

Fig. 8 Typical On-Line Data Record

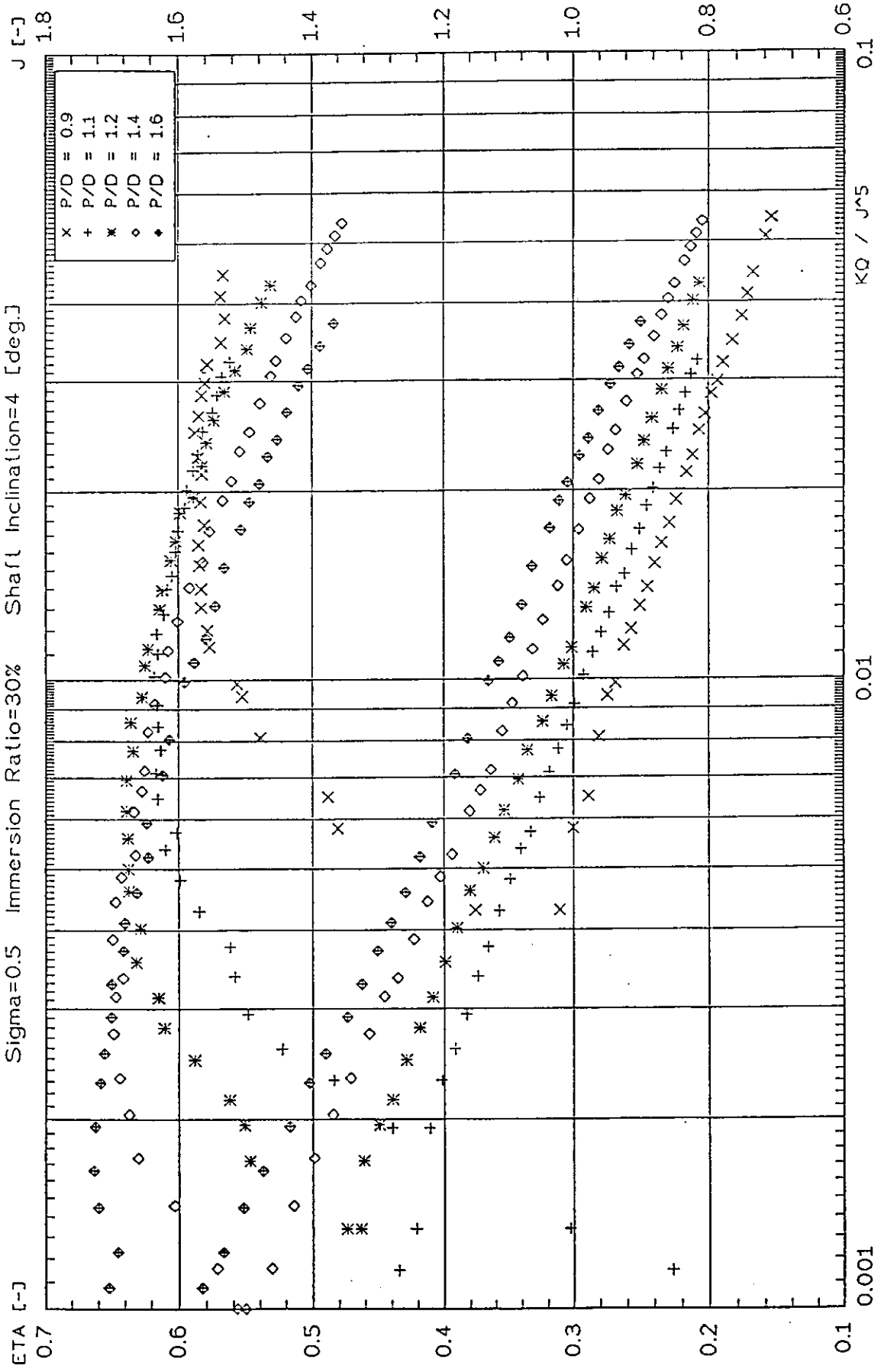

Fig. 9 Design Chart for Small Shaft Angle

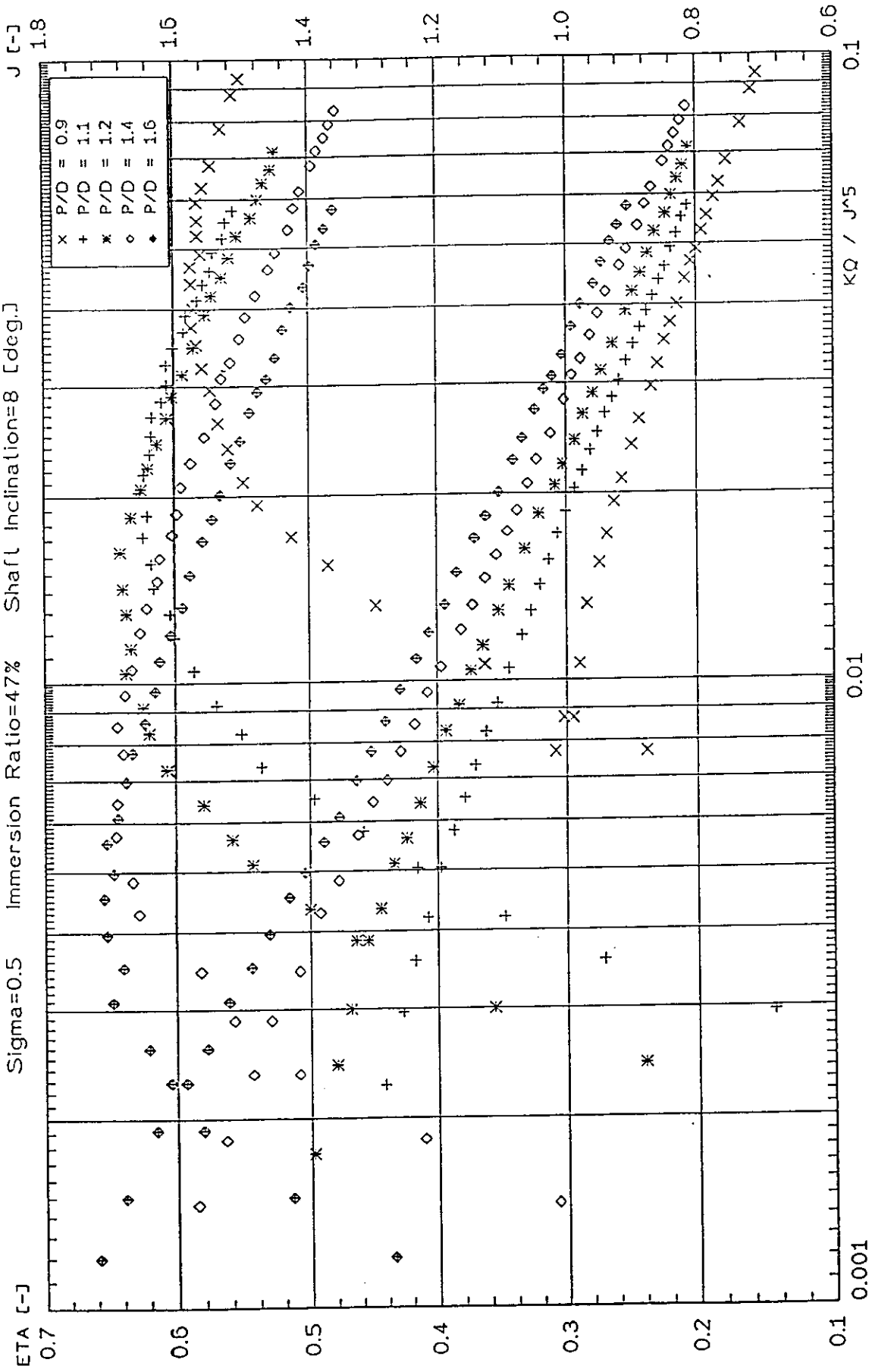

Fig. 10 Design Chart for Mean Shaft Angle

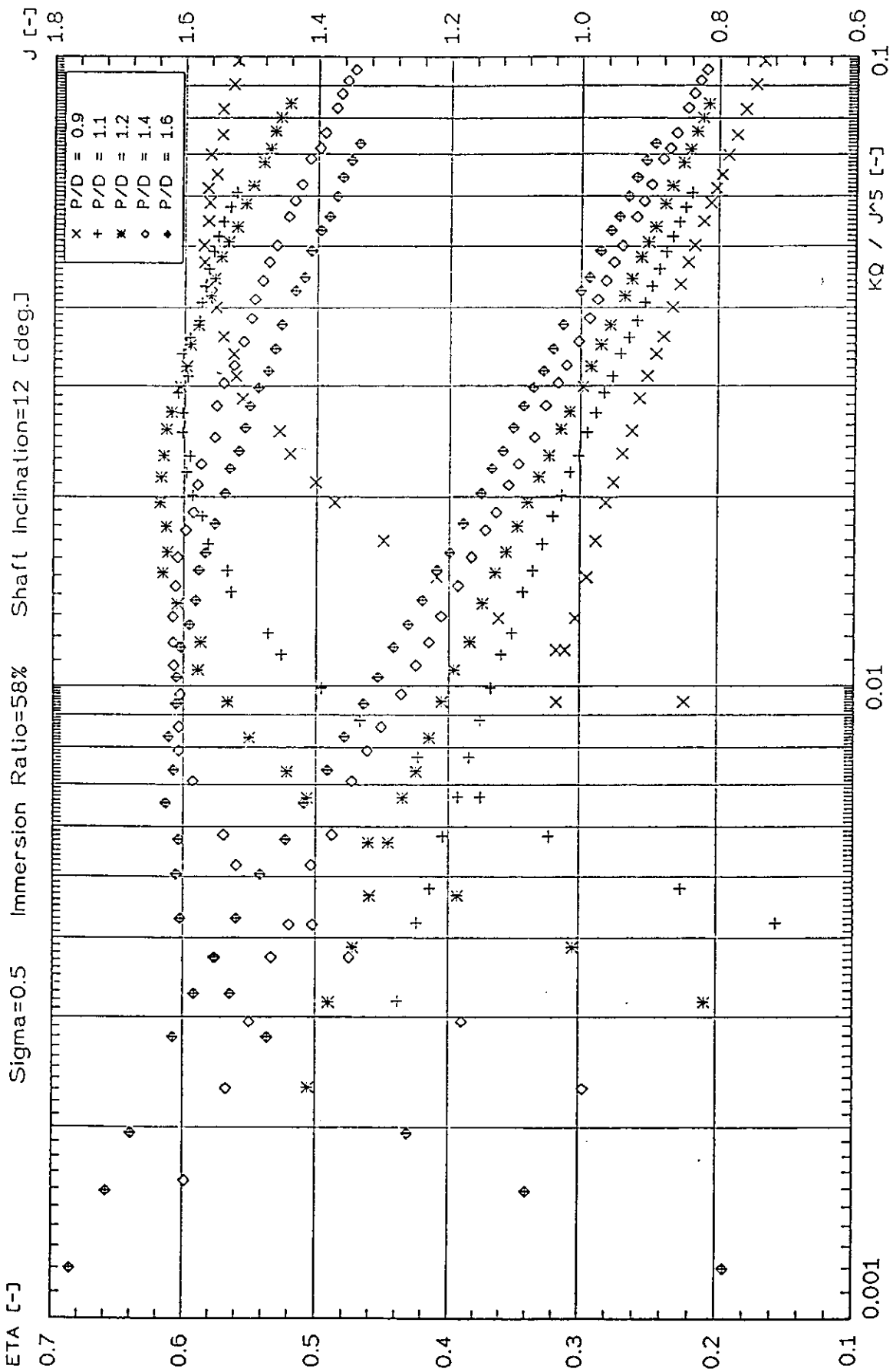

Fig. 11 Design Chart for Large Shaft Angle

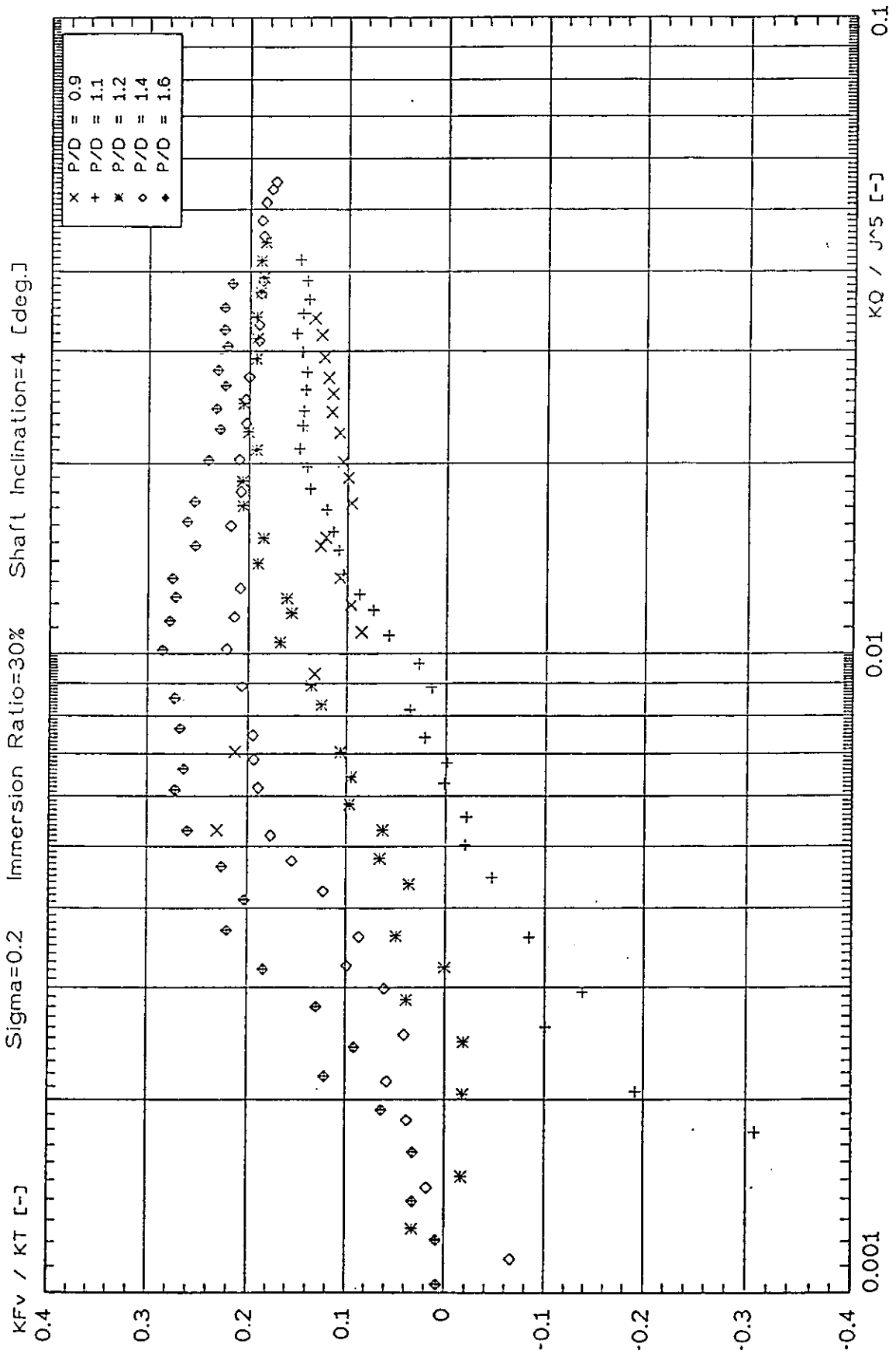

Fig. 12 Propeller Lift Forces for Small Shaft Angle

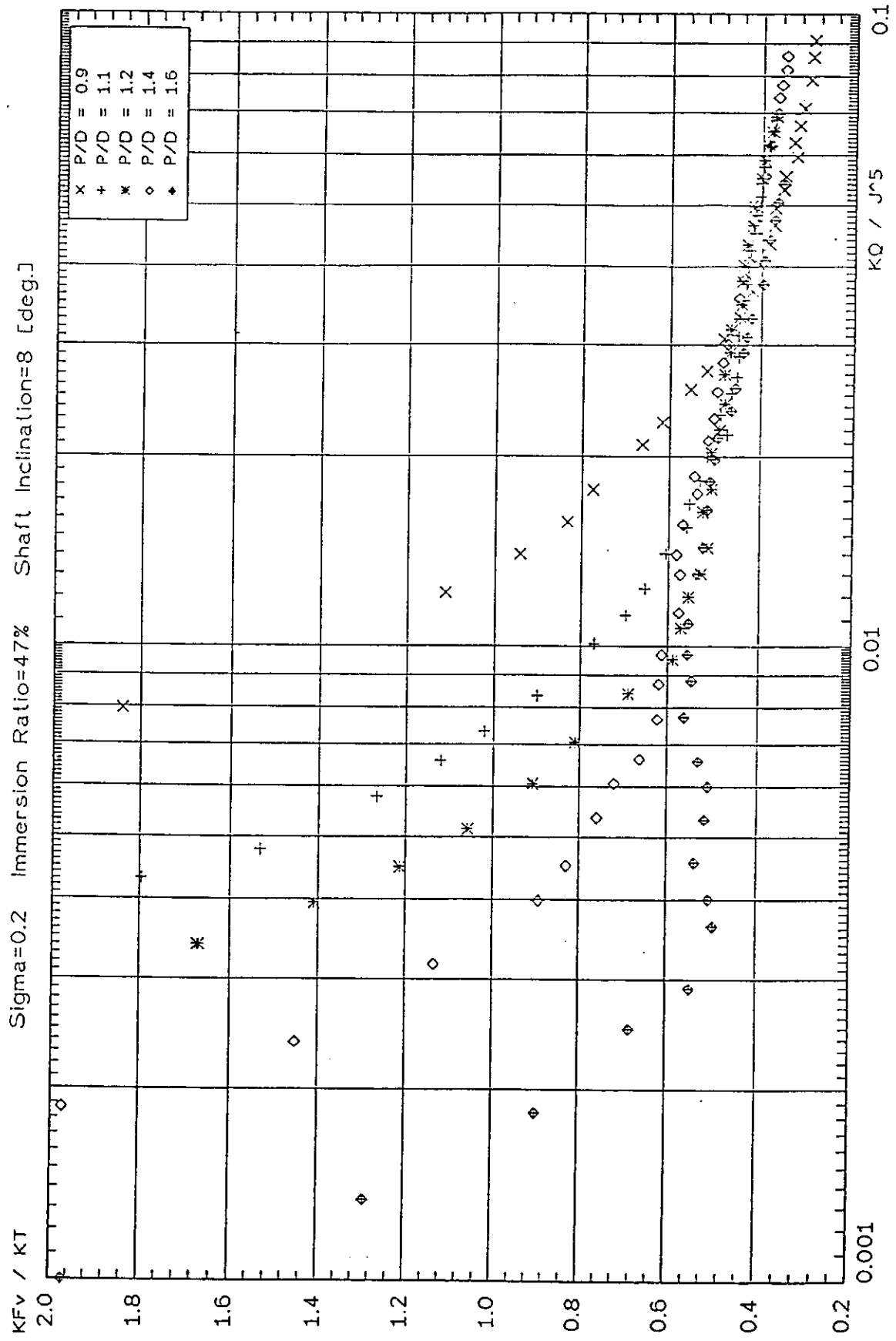

Fig. 13 Propeller Lift Forces for Mean Shaft Angle

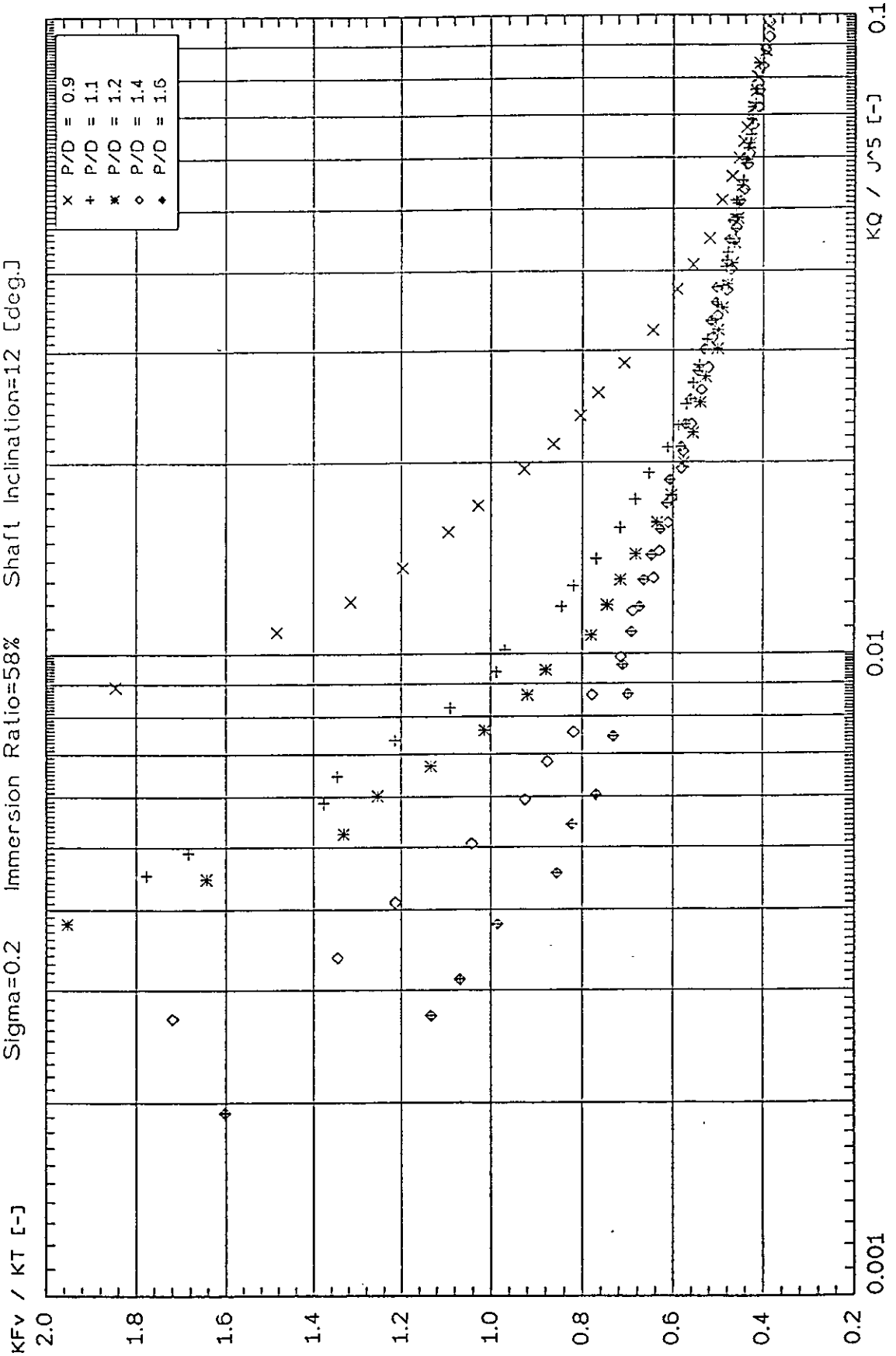

Fig. 14 Propeller Lift Forces for Large Shaft Angle

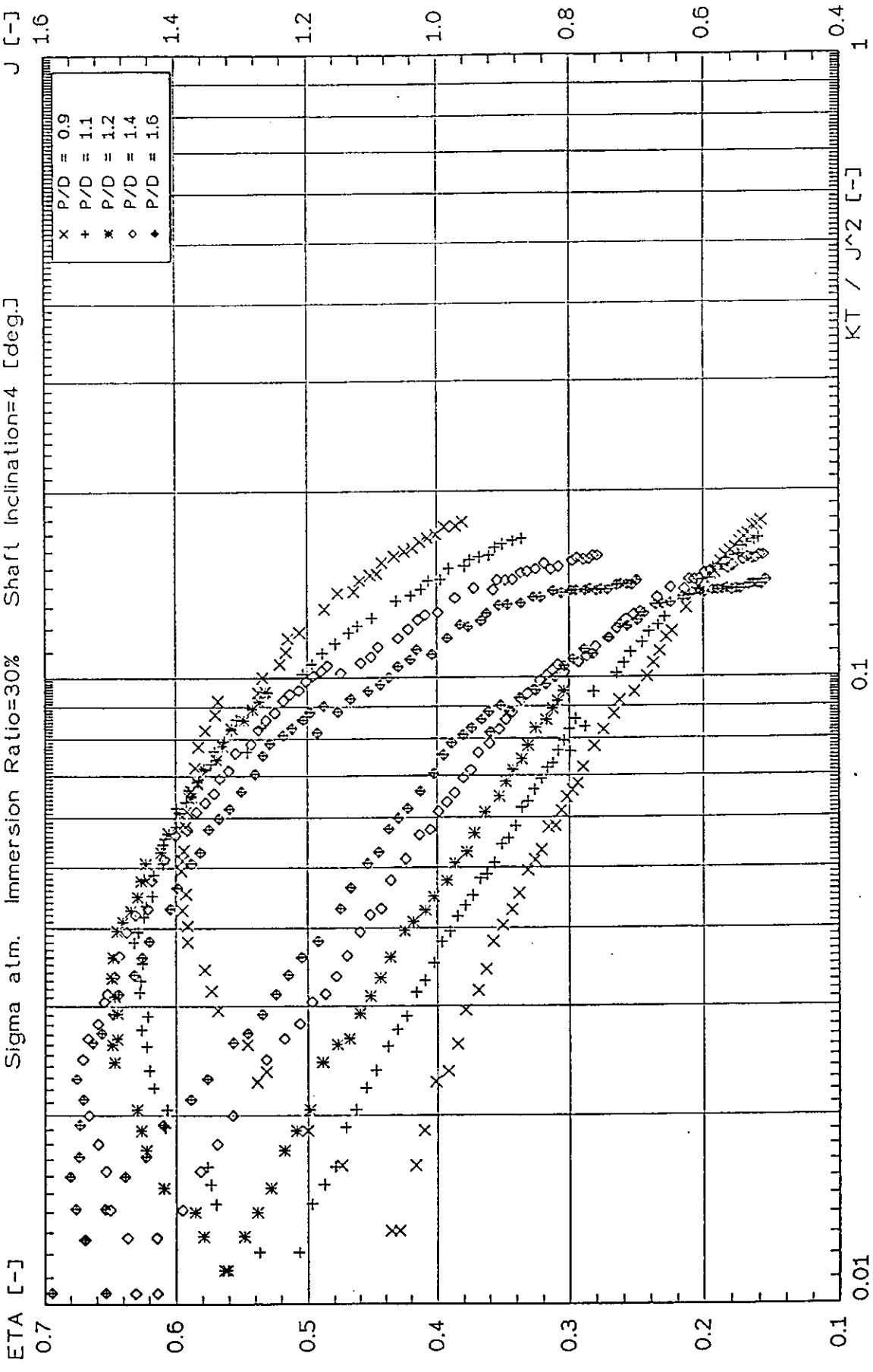

Fig. 15 Thrust Loading Capacity for Small Shaft Angle

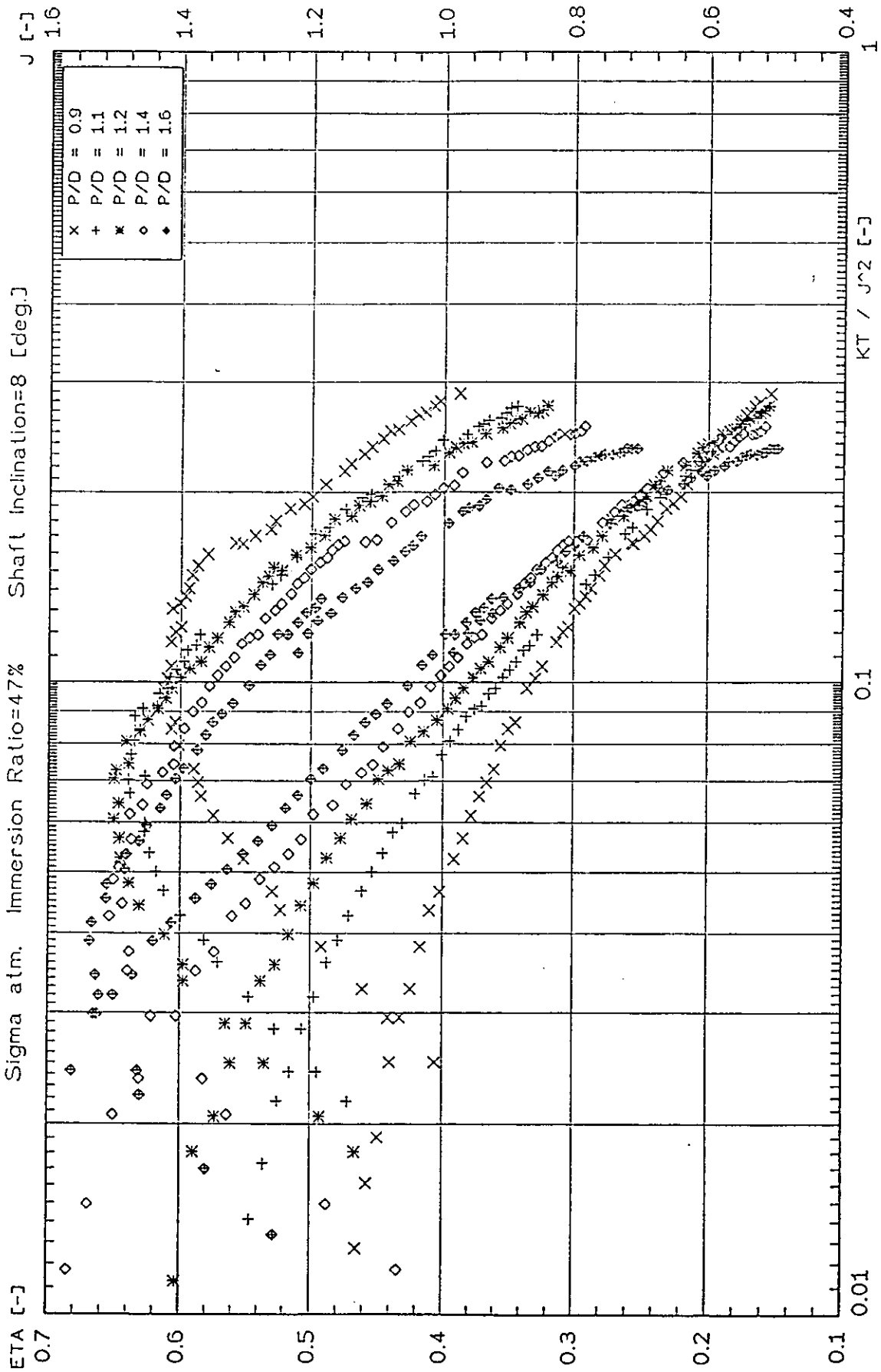

Fig. 16 Thrust Loading Capacity for Mean Shaft Angle

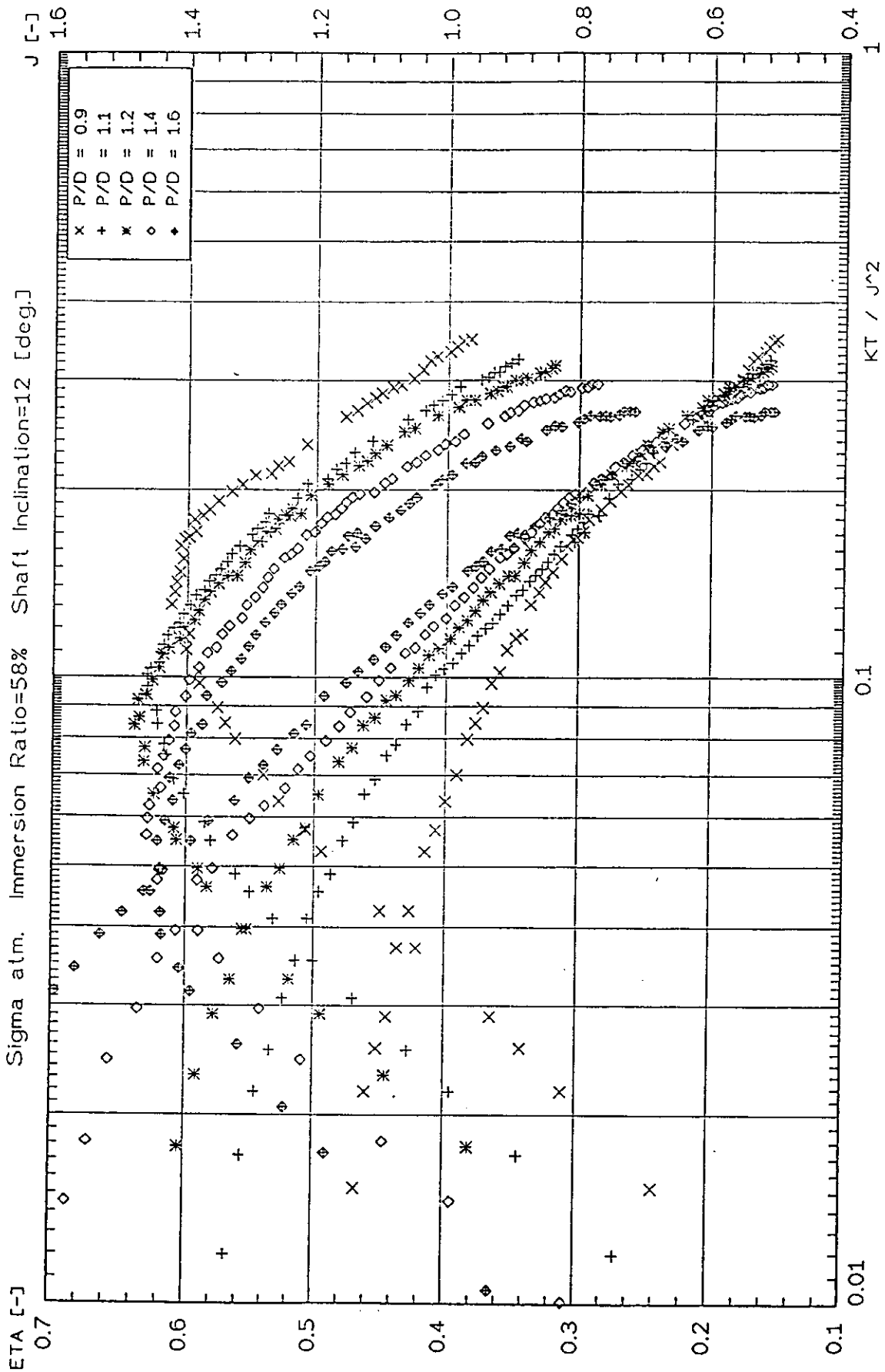

Fig. 17 Thrust Loading Capacity for Large Shaft Angle

Attention should also be drawn to the aspect of thrust limitations known to be somewhat critical in certain applications of surface piercing propeller systems. For the propeller series investigated one can deduce from Fig. 15 that for small immersion ratios and small shaft angles thrust loading coefficients of $K_T/J^2 = 0.20$ are probably the maximum achievable limit, if the pitch-diameter ratio is small. If propeller immersion is increased by means of running at higher shaft angles it looks as if thrust loading coefficients of about $K_T/J^2 = 0.35$ can be achieved, again at small pitch-diameter ratios (see Fig. 17). For fixed pitch propellers with high pitch-diameter ratios the achievable thrust loading in terms of K_T/J^2 is obviously much smaller. Controllable pitch propellers may be a solution to all problems of this nature, but possible disadvantages of their larger hub-diameter ratios have not been the subject of a referrable investigation yet.

5. ACKNOWLEDGEMENT

The authors wish to thank Philip Rolla of *Rolla SP Propellers SA*, Switzerland for his permission to publish the results of this investigation. The authors are certain that in this way the hydrodynamics of surface piercing propellers will become better understood in the marine community, which in turn will be beneficial for their application and success in high-speed craft.